Journal of Food Composition and Analysis 136 (2024) 106740

Contents lists available at ScienceDirect

Journal of Food Composition and Analysis

journal homepage: www.elsevier.com/locate/jfca

Rapid detection of benzoic, sorbic, and dehydroacetic acids in processed foods using surface-enhanced Raman scattering spectroscopy

Ching-Wei Yu [a], Chao-Ming Tsen [b], Sz-Ying Chen [b], Zi-Ting Yang [b], Yi-Jun Jen [a,*]

[a] Department of Electro-Optical Engineering, National Taipei University of Technology, No. 1, Section 3, Chung-Hsiao E. Rd., Taipei 106344, Taiwan
[b] Residue Control Division, Agricultural Chemicals Research Institute, Ministry of Agriculture, Executive Yuan, No.11, Guangming Rd., Wufong, Taichung 41358, Taiwan

ARTICLE INFO

Keywords:
Surface enhanced Raman scattering
Marangoni flow
Benzoic acid
Sorbic acid
Dehydroacetic acids
Processed foods

ABSTRACT

Benzoic acid (BA), sorbic acid (SA), and dehydroacetic acid (DHA) are among the most common food additives that are classified as antimicrobial preservatives. However, their consumption in excess can lead to damage to the human liver and kidneys. At the present time, no rapid method has been developed for the simultaneous detection of these preservatives in processed foods. In this study, an expedited process based on surface-enhanced Raman scattering (SERS) and solid-phase extraction (SPE) has been developed to determine the content of the preservatives in processed seafood, minced fish, and cheese products. The effect of local heating on SERS spectra at the center of the droplet, which was deposited onto silver nanopillar arrays used as the SERS substrate, was examined. A recirculating flow, manifested as twin vortices merging within the droplet, brought the preservative molecules down to the droplet's center, resulting in an increase in the SERS signals. Furthermore, the screening efficiency of the detection method for the three preservatives was experimentally evaluated in real samples. The experimentally determined Raman bands of the added BA, SA, and DHA were compared with amounts obtained by the conventional method of high-performance liquid chromatograph (HPLC).

1. Introduction

Benzoic acid (BA), sorbic acid (SA), and dehydroacetic acid (DHA) are among the most common food additives. These are classified as antimicrobial preservatives and are used in food processing to extend shelf life and prevent decomposition caused by microbial growth (Alagöz et al., 2015; Lone et al., 2023; Mejlholm et al., 2008; Mejlholm and Dalgaard, 2013). Salt formation, which includes compounds such as sodium benzoate, sodium sorbate, potassium benzoate, potassium sorbate, calcium sorbate, and sodium dehydroacetate, is frequently employed to enhance the solubility of BA, SA, and DHA in water. These preservatives are commonly added to processed seafood and minced fish products, which are rich in proteins. However, the Food and Drug Administration (FDA) in each country sets the maximum residue limits (MRLs) of these preservatives in food. Overconsumption of BA, SA, and DHA can lead to damage in the human liver and kidneys, and may even cause toxic reactions (Dong and Wang, 2006). The conventional method for performing quantitative analysis of the preservatives (Amirpour et al., 2015; Mologni et al., 2016; Saad et al., 2005; Sirhan, 2018) involves the use of a high-performance liquid chromatograph (HPLC) coupled with a photodiode array detector. Since the method requires an expensive instrument, is time-consuming, and involves complicated sample pretreatments in a laboratory environment, it becomes difficult to conduct on-site quality control of raw materials in food processing factories, restaurants, and supermarkets. The risk of the excessive and illegal addition of BA, SA, and DHA to processed foods is high due to the lack of an on-site inspection method.

BA is characterized as a typical aromatic monocarboxylic acid, while SA is an unsaturated monocarboxylic fatty acid with a straight chain (Gao et al., 2013, Kai et al., 1989). Pagannone et al. found that BA, comprising a benzene ring core and that carries a carboxylic acid substituent, may be absorbed on a metal surface forming a bidentate bridging structure (Pagannone et al., 1987). Kai et al. conducted an examination of the multiple absorption states of SA and identified the band feature of the Raman spectrum of silver sols (Kai et al., 1989). SA is a hexadienoic acid with four geometrical isomers and reaction involves the attachment of its carboxyl group to the metal. The adsorption behavior and mechanism of BA and SA on the surfaces of metal nanostructures has been investigated using density functional theory (Choi and Park, 2005, Saraiva et al., 2015, Zhao and Fang, 2006).

* Corresponding author.
E-mail addresses: chingwei13@gmail.com (C.-W. Yu), cmtsen@acri.gov.tw (C.-M. Tsen), ssein93@acri.gov.tw (S.-Y. Chen), z600000tw@gmail.com (Z.-T. Yang), jyjun@ntut.edu.tw (Y.-J. Jen).

https://doi.org/10.1016/j.jfca.2024.106740
Received 23 July 2024; Received in revised form 4 September 2024; Accepted 10 September 2024
Available online 13 September 2024

Additionally, DHA contains carbonyl groups and exists in five tautomeric forms. The Raman spectrum of DHA was measured and the assignments of the vibrational bands were identified based on quantum chemical calculations (Billes et al., 2015).

Surface enhanced Raman scattering (SERS) is a Raman-based technique that holds promise for the chemical analysis of food (Cai et al., 2024, Feng et al., 2024, Ma et al., 2024, Neng et al., 2023, Qi et al., 2024, Zhang et al., 2023). It has emerged as a potent analytical tool for the identification of additives across a broad spectrum of food products (Cai et al., 2018, Hussain et al., 2020, Luo et al., 2018, Yang et al., 2022). Lei et al. conducted measurements of the SERS spectra of BA, which was absorbed on a thin layer of silver nanocrystals, at several excitation wavelengths (Lei et al., 1995). The enhancement achieved from a silver nanocrystal with a mean grain size of 15 nm surpassed that obtained from an isotropic silver film in the attenuated total reflection configuration. Gao et al. fabricated gold nanoparticles with an approximate diameter of 13 nm, using them as a SERS substrate to amplify the Raman scattering of BA. This was achieved with an He-Ne laser at a wavelength of 632.8 nm (Gao et al., 2013). However, a large Raman enhancement can be achieved by binding specific molecules onto the surface of plasmonic metal films, such as bideposited silver nanocolloid arrays (Jen et al., 2020), gold nanohelx arrays (Jen et al., 2010, Jen et al., 2016) and silver nanorods (Chu et al., 2007, Jen et al., 2012, Jen et al., 2019). The localized surface plasmon resonance (Fang et al., 2020, Pelle et al., 2018, Shrivas et al., 2018) induced by nano-scale metal films can significantly increase the local electric-field intensity in a hot spot. A significant Raman enhancement factor for silver nanorod arrays has been demonstrated through the measurement of the SERS spectrum of Rhodamine 6 G, when it is diluted in an organic solvent. Owing to its great effectiveness for rapid inspection, a SERS-based sensor has been achieved for the dithiocarbamate pesticide residues in agriculture (Tsen et al., 2021). The extraction procedure for removing ingredients from adzuki beans was developed, and a SERS spectrum of paraquat was obtained on an agricultural site (Tsen et al., 2018).

Despite its advantages such as minimal sample preparation, short detection time, high sensitivities, and resistance to water interference, SERS generally encounters challenges with signal suppression by certain ingredients in processed foods, including proteins, salts, lipids, and organic substances. In this study, a rapid method for the determination of three kinds of preservatives, BA, SA, and DHA in processed foods was developed using SERS combined with solid-phase extraction (SPE). The effect of local heating at the center of the droplet from the eluting fraction deposited on the silver nanopillar arrays was investigated using a 785 nm laser operating in continuous wave (CW) mode. A temperature gradient was formed on the surface of the drop and may induce surface tension driven Marangoni (Diddens et al., 2021, Askounis et al., 2017). The formation of Marangoni flows manifested the twin vortices merging within the droplet and therefore led to the concentration of the preservatives and an increase of SERS.

Processed food could be considered a complex multifluorophoric system, containing several compounds such as phospholipids, proteins, peptides, and free amino acids (Aubourg and Medina, 1997; Aubourg et al., 1998; Hassoun et al., 2019). Fluorescence is an undesirable side effect found in Raman spectra. Most of the interference from non-target compounds in foods could cause fluorescence spectra in the visible to near-infrared wavelength range. However, after the wash and elution steps from the SPE clean-up procedure, the undesired fluorescence background was reduced. Nevertheless, the extracts from the eluting fraction still contain parts of the complex matrices and interfere with the desired Raman signals. When the droplet of the eluting fraction was deposited onto silver nanopillars, the remaining complex matrices, such as lipids and proteins, would competitively cover the metallic surface, isolating it from the preservative molecules. Consequently, the minor amounts of preservatives binding to the metallic surface result in weaker SERS signals. In order to increase the binding probability between the molecules and the surface, local heating with a 785 nm laser was applied to the substrate before the complex matrices completely covered it. Twin vortices within the droplet were coincidentally induced, bringing the preservative molecules to the droplet's center and causing them to adhere to the laser spot area. When the metallic film was continuously illuminated with the laser, the adsorption kinetics of the molecules to the metallic surface increased, resulting in a faster rate of adsorption (Olson and Harris, 2008). The increase in signal was attributed to the electromagnetic enhancement mechanism (EEM) (Moskovits, 1985; Stiles et al., 2008), where the SERS signals of the molecules can be significantly enhanced when they are within several molecular lengths of the metal. The method we propose here not only provides the simple procedure for detecting the preservatives in processed foods, but also mitigates the SERS suppression from food ingredients. Furthermore, the screening efficiency of the detection method for the three preservatives was experimentally evaluated in processed seafood, minced fish, and cheese products. The experimentally determined Raman bands of the added BA, SA, and DHA were compared with amounts obtained by the conventional method of HPLC.

2. Material and methods

2.1. Samples

In this study, 50 samples, composed of different types of minced fish, processed seafood, and cheese products, were directly purchased from a supermarket (PX Mart, TW). The following samples were collected and analyzed: 20 minced fish products (including 2 fish paste, 2 fish dumpling, 2 crab stick, 3 tempura, 3 kamaboko, 2 milkfish ball, 1 cod ball,1 fish ball, 1 sailfish ball, 1 salmon ball, 1 fish roe roll, and 1 caviar ball); 10 seafood products (including 3 cuttlefish ball, 1 cuttlefish dumpling, 1 cuttlefish shrimp ball, 1 octopus kamaboko, 1 shrimp ball, 1 shrimp dumpling, 1 squid ball, and 1 squid paste); 20 cheese products (3 Cheddar cheese, 4 Mozzarella cheese, 1 Gouda cheese, 1 truffle cheese, 1 Emmental cheese, 1 sweet potato cheese, 1 Parmesan cheese, 8 process cheese). Upon arrival at the laboratory, the samples were stored at $-18\ ^{\circ}C \pm 2\ ^{\circ}C$. Prior to measurement, frozen samples were removed from the freezer and allowed to warm to room temperature.

2.2. Reagents and materials

Sodium benzoate (99 %), potassium sorbate (99 %), sodium dehydroacetate (99 %), and rhodamine 6 G (R6G, 99 %) were purchased from Merck KGaA (Darmstadt, Germany). Methanol (MeOH; LC-MS grade) was purchased from Roth (Karlsruhe, Germany). Reagents included deionized water (DI H_2O; resistivity $\geq$ 18 MΩ • cm at 25°C), DI water-methanol solution (2:8, V/V, DI H_2O/MeOH), DI water-methanol solution (1:1, V/V, DI H_2O/MeOH) and DI water-methanol solution (8:2, V/V, DI H_2O/MeOH). All chemicals were used without further purification. Stock solutions of benzoic and sorbic acid standards were prepared by dissolving 10 mg of the sodium benzoate and the potassium sorbate in 2 mL of deionized water with sonication for 5 minutes, respectively. A stock solution of dehydroacetic acid standard was prepared by dissolving 10 mg of the sodium dehydroacetate in 2 mL of deionized water with sonication for 5 minutes. Subsequently, the standard stock solutions were diluted by adding DI water-methanol solution (1:1, V/V, DI H_2O/MeOH) to prepare each desired concentration of standard samples in the mobile phase. Additionally, a stock solution of R6G was prepared by dissolving 50 mg of the standard in 0.5 mL of methanol with sonication for 5 minutes and diluting by adding water-methanol solution (1:1, V/V, DI H_2O/MeOH) to the desired concentration. All stock solutions of the preservatives were stored at 4°C before measurement.

2.3. Sample pretreatment

Two grams of homogenized sample was added 5 mL DI water-methanol solution (1:1, V/V, DI H_2O/MeOH) in a 15 mL centrifuge

tube. The food sample was mixed thoroughly with the extraction solution by shaking the tube for 1 minute; the mixtures was then allowed to stand for 3 minutes. A solid-phase extraction cartridge (PT-001/3 mL volume; GETECH, Taiwan) was used to retain the BA, SA, and DHA molecules on the filling sorbents before the elution step. Prior to the use of the cartridge a 2 mL DI water-methanol solution (1:1, V/V, DI H_2O/MeOH) passes through the cartridge as a condition solvent. A 200 μL volume of the supernatant was passed through the SPE cartridge. The cartridge was then washed with 600 μL DI water-methanol solution (8:2, V/V, DI H_2O/MeOH) at a flow rate of one drip per second to remove impurities. The preservatives BA, SA, and DHA were eluted with a 400 μL DI water-methanol solution (2:8, V/V, DI H_2O/MeOH) at a flow rate of one drip per second. The eluting fraction was collected and stored as a test solution for further SERS analysis.

2.4. Fabrication of SERS substrate

Glancing Angle Deposition (GLAD), a technique that involves physical vapor deposition, requires the substrate stage to be tilted at an angle, θv, which is between the normal of the substrate and the incoming vapor flux (Liu et al., 2010, Robbie et al., 2004). During the initial deposition, nucleation centers form randomly on the bare silicon substrate. The subsequently deposited flux then causes the preferential growth of metal nanorods towards the direction of deposition due to the shadowing effect. The deposition angle was kept large to achieve metallic film porosity and appropriate column spacing. A set chamber pressure of 2×10^{-6} Torr was reached prior to the silver deposition. Silver particles with a purity of 99.99 % were used as the vapor source in the electron-beam evaporation system. In the fabrication of the silver nanopillar arrays as the SERS substrate, the angle of θ_v was set at 86° and the deposition rate was controlled at approximately 0.5 nm/s. The substrate was rotated about its normal at a rate of 10 rpm simultaneously during the deposition process. The thickness of the film was monitored by measuring the mass of the evaporated silver using a quartz crystal microbalance. Figures A.1 (a) and (b) show the cross-sectional and top-view scanning electron microscopy (SEM) images of the silver nanopillar arrays, respectively. The cross-sectional SEM image reveals the morphology of the nanostructures with a thickness of 150 ± 10nm. The analytical enhancement factor (AEF) of the SERS substrate could be estimated from the standard equation as follows (Jen et al., 2020):

$$AEF = \frac{I_{SERS}N_{bulk}}{I_{bulk}N_{SERS}} \quad (1)$$

where I_{SERS} and I_{bulk} are the Raman intensity of the specific band of the analyte adsorbed on the SERS substrate and the bulk analyte itself, respectively. N_{bulk} and N_{SERS} are the number of molecules on the substrate and that in the bulk, respectively. The AEF was then determined to be 1.61×10^6 for a R6G molecule at the band of 1502 cm^{-1} (Vosgröne and Meixner, 2005) using a Raman spectrometer with a wavelength of 785 nm.

The SERS substrate, comprising randomly distributed silver nanopillar arrays, exhibits broad absorbance spectra for both p- and s-polarizations in the wavelength range of 400 nm to 950 nm, as shown in Fig. A.2 (a) and (b), respectively. As we know, the SERS enhancement is related to the two-fold EEM that involves the absorbance of incident excitation and Raman-scattered light (Kumar et al., 2020). Compared with previous studies (Kumar et al., 2022, Waiwijit et al., 2020) on GLAD-based SERS substrates that exhibit anomalous absorbance properties, such as aligned metallic nanorods, the silver nanopillar arrays present stronger absorbance, exceeding 0.8 (80 % in absorption), in the range of Raman-scattered wavelengths (800 nm – 900 nm) and at the excitation wavelength of 785 nm for both polarizations. The absorbance for the wavelengths at which the Raman signals occur is slightly higher than that at 785 nm wavelength. Therefore, the SERS bands were significantly enhanced due to the non-polarization-dependent absorbance spectra of the substrate. Additionally, there is another way to achieve the high absorbance spectra of SERS substrates, which is by depositing silver nanostructures on an anisotropic dielectric layer thin-film (Kumar et al., 2020, Lin et al., 2024). However, when the multi-layered film was constantly illuminated by an excitation laser at a power of over 10 mW, thermally-induced structural damage appeared at the position of the laser focusing spot (Lin et al., 2024), and the SERS enhancement decreased rapidly. In contrast, the SERS substrate proposed in this study can withstand high-powered illumination of over 30 mW using a 785 nm continuous wave laser, achieving a local heating effect on the SERS spectra of preservatives prior to measurement. The substrate comprising silver pillar arrays boasts easy processing on a large scale (compared to multi-layered films), high absorbance properties for both p- and s-polarizations (over 0.8 at excitation and Raman-scattered wavelengths), and excellent SERS enhancement at a 785 nm excitation.

2.5. Instruments and detection method

Raman spectra of the food samples were obtained using a portable Raman spectrometer (RMS-1000, Oceanhood Inc., Zhongli, TW) with a 785 nm laser source. The resolution of the spectrometer was 12 cm^{-1} and the focal length of the objective was 7.5 mm±0.5 mm. Instrument parameters were set as follows: integration time of 2 seconds and 50 mW laser power. All measured spectra were baseline-subtracted using adaptive iteratively reweighted Penalized Least Squares algorithm (Zhang et al., 2010). A silver film comprising nanopillar arrays was used as the SERS substrate to detect the preservatives in foods. The schematic illustration of the principle of detecting preservatives based on SERS and SPE is shown in Fig. 1. The sample extracts were processed using PT-001 SPE via the procedure described in Section 2.3. After the wash and elution steps from the SPE clean-up procedure, a purified sample aliquot was collected and gently deposited on the SERS substrate with an area of 2.2 mm × 2.2 mm. When the droplet of the eluting fraction was deposited onto silver nanopillars, the remaining complex matrices, such as lipids, peptides, and proteins, would competitively cover the metallic surface. The preservative molecules could not directly contact the metallic surface of the substrate, resulting in a weak Raman signal from the molecules. However, when the droplet was initially illuminated by a 785 nm CW laser prior to spectra acquisition, the resulting Raman signal was significantly enhanced. The laser light was focused onto the substrate using a 5× objective, and the laser power was kept constant at 30 mW. A temperature gradient was formed on the surface of the drop, which may induce surface tension-driven Marangoni flows (Diddens et al., 2021, Askounis et al., 2017). The formation of Marangoni flows manifested the twin vortices and led to the concentration of the preservative molecules at the center of the drop. On the other hand, center heating could improve the binding probability between the silver nanopillars and the preservatives, resulting in significant Raman signal enhancement.

3. Results

3.1. Local heating effect on SERS spectra

3.1.1. Contact angles of droplet

Samples of cuttlefish ball, spiked with a concentration of 1.0 g/kg of SA, were prepared. The extracts from these samples were processed using an SPE cartridge, following the procedure mentioned in Section 2.3. The eluting fraction collected into a 1 mL vial glass was then mixed with 200 μL DI water. The SERS substrate, which comprises silver nanopillar arrays, was cut into a square with an area of 2.2 mm × 2.2 mm before the mixture was dropped onto it. Fig. 2 presents the SERS spectra of the spiked samples, with different drop volumes of 1.5, 3.0, 4.5 and 7.5 μL gently deposited on the substrate. Visualization of the contact angles θ_c between these drops and the substrate showed them to

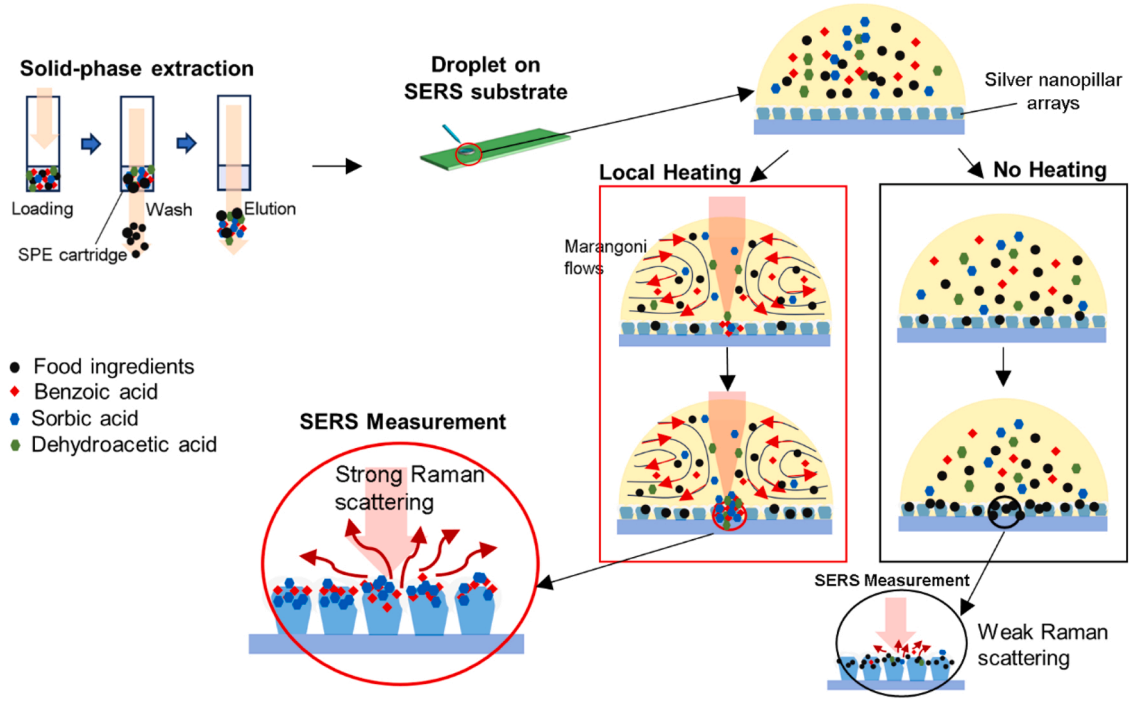

Fig. 1. Schematic illustration of the principle of detecting preservatives based on surface-enhanced Raman scattering (SERS) and solid-phase extraction (SPE). Local heating was performed at the center of droplet deposited on the substrate before the SERS measurement.

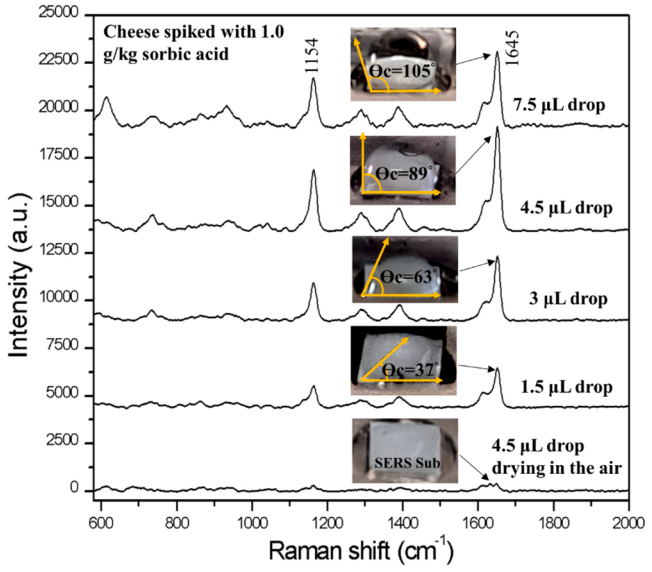

Fig. 2. SERS spectra of the spiked cuttlefish ball, with different drop volumes of 1.5, 3.0, 4.5 and 7.5 μL gently deposited on the SERS substrate. The size of the substrate comprising the silver nanorod arrays was 2.2 mm × 2.2 mm area and the concentration of SA was 1.0 g/kg.

be 37°, 63°, 89°, and 105°, respectively. Local heating was performed at the center of the substrate for each drop using a 785 nm CW laser with 30 mW for 15 seconds prior to the measurement. The results indicated that, among the drops tested, the one with a volume of 4.5 μL has the greatest Raman signals of SA bands at 1154 and 1645 cm^{-1}. A temperature gradient formed on the droplet's surface due to heat conduction through the substrate during laser heating. This induced a recirculating flow, manifested as twin vortices merging within the droplet, which brought the preservative molecules down to the droplet's center. When the contact angle was significantly less than 90°, the twin vortices split, preventing the molecules from concentrating at the center. Furthermore, a large contact angle resulted in a high curvature at the droplet's apex. This caused the laser to defocus from the surface of the substrate, which subsequently led to a decrease in SERS. Another common method involves drying the droplet on the substrate in the air before measurement. Despite the sample being pretreated, the complex residue from the sample matrices covers the surface of the SERS substrate. This prevents the molecules from binding to it, thereby suppressing the SERS signal.

3.1.2. *Influence of heating period*

In order to investigate the local heating effect on the SERS spectra of preservatives in processed foods, we prepared three samples of cuttlefish ball. These were spiked with a concentration of 0.5 g/kg of BA, SA, and DHA, respectively. The sample pretreatment was performed and the eluting fraction was mixed with 200 μL DI water. The droplet volume of 4.5 μL was gently deposited on the SERS substrate prior to the laser heating. The power of the laser operating in CW mode was kept at 30 mW. The spectra were captured immediately after the heating was finished, with an integration time of 2 seconds and a power of 50 mW. Fig. 3(a) to (c) show the measured spectra of the spiked sample versus different heating period for BA, SA, and DHA, respectively. The results indicate that the Raman signals of the preservatives increased during the heating period, which ranged from 0.5 seconds to 15 seconds. As depicted in Fig. 3(a), the measured SERS spectra display Raman bands of BA at 845 cm^{-1}, 1002 cm^{-1}, and 1595 cm^{-1}, recorded at the 0.5, 5, and 15-second mark. The vibration bands of BA are related to the in-plane ring breathing and the C–C stretching modes at around 1002 cm^{-1} and 1595 cm^{-1}, respectively. The band at 845 cm^{-1} is attributed to the COO^- in-plane scissoring vibration mode (Gao et al., 2013). The measured SERS spectra exhibit the strongest intensity of the BA bands recorded at the 15-second mark. A similar tendency was observed in that the Raman bands of SA and DHA increased with the heating period, as shown in Fig. 3(b) and Fig. 3(c). The measured SERS spectra exhibit the strongest intensity of the SA bands at 1154 cm^{-1} and 1645 cm^{-1} and the strongest intensity of the DHA bands at 631 cm^{-1}, 705 cm^{-1}, 940 cm^{-1}, 1239 cm^{-1}, 1378 cm^{-1}, and 1637 cm^{-1}, recorded at the 15-second

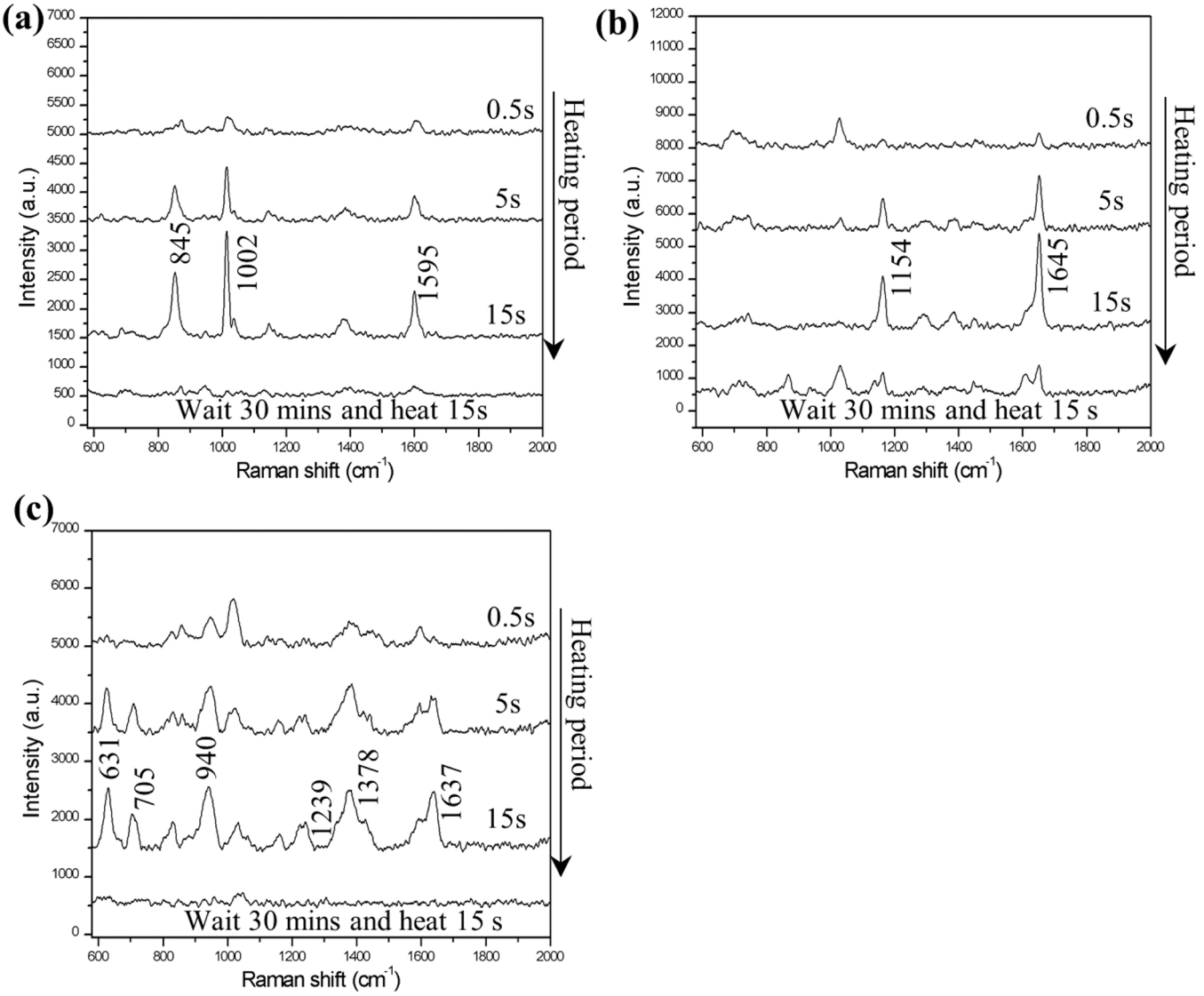

Fig. 3. SERS spectra of spiked cuttlefish ball with a concentration of 0.5 g/kg of (a) BA, (b) SA, and (c) DHA recorded at the 0.5, 5, and 15-second mark. The droplet volume was 4.5 μL and the power of a CW laser heating at the center of the droplet was kept at 30 mW before SERS measurement.

mark. The vibration bands of SA at 1645 cm^{-1} arise from either C–C or C–O stretching modes (Saraiva et al., 2015). The band at 1154 cm^{-1} is associated with a combination of bending motions of the molecular skeleton of the sorbic acid. The bands of DHA at 631 cm^{-1} to 1378 cm^{-1}, and at 1637 cm^{-1}, arise from either C–C stretching or C–C in-plane deformation modes (Billes et al., 2015). The Raman bands of the three preservatives coincided with the standard reference.

According to a previous study (Olson et al., 2008), when the metallic film was continuously illuminated with the laser, the kinetics of adsorption of a surfactant molecule to the metallic surface increased, resulting in a faster rate of adsorption and an increased Raman signal. However, when the droplet from the eluting fraction containing complex matrices of foods was deposited onto the metallic SERS substrate, the preservative molecules could not directly contact the metallic surface of the substrate, and the binding probability between the silver nanopillars and the preservatives dropped significantly. As shown in Fig. 3, the Raman bands of the measured SERS spectra for three preservatives were weak at the 0.5-second mark. When the droplet was deposited onto the substrate and left in the air for 30 minutes, the intensity of the Raman bands of the three preservatives did not increase despite the illumination of laser heating. This is because the complex matrices, such as lipids and proteins, from the food sample first occupied the metallic surface of the substrate, preventing the preservatives from binding to the surface. In contrast, when local heating with a 785 nm laser at 30 mW power was initially applied to the droplet for the first 15 seconds, twin vortices merging within the droplet were induced, bringing the preservative molecules down to the laser spot area. The binding probability between the molecules and the surface improved, and an increase in the band intensities of the preservatives was observed. The increase in signal was attributed to the EEM, where the molecules can be significantly enhanced when they are within several molecular lengths of the metal.

3.2. *Eluting fractions from SPE with the PT-001 SPE cartridge*

To enable the SERS measurement of trace amounts of three preservatives in the food matrix, the eluting fractions collected from the PT-001 SPE were investigated. We prepared samples of cuttlefish ball, each spiked with a concentration of 0.5 g/kg of BA, SA, and DHA. Fig. 4(a) depicts the intensity of the dominant bands of three preservatives, which were eluted with a 400 μL DI water-methanol solution (2:8, V/V) from the SPE cartridge, as a function of the heating period. This period ranged from 0.5 seconds to 25 seconds. The eluting fraction was mixed with 200 μL DI water before depositing onto the substrate. The laser power

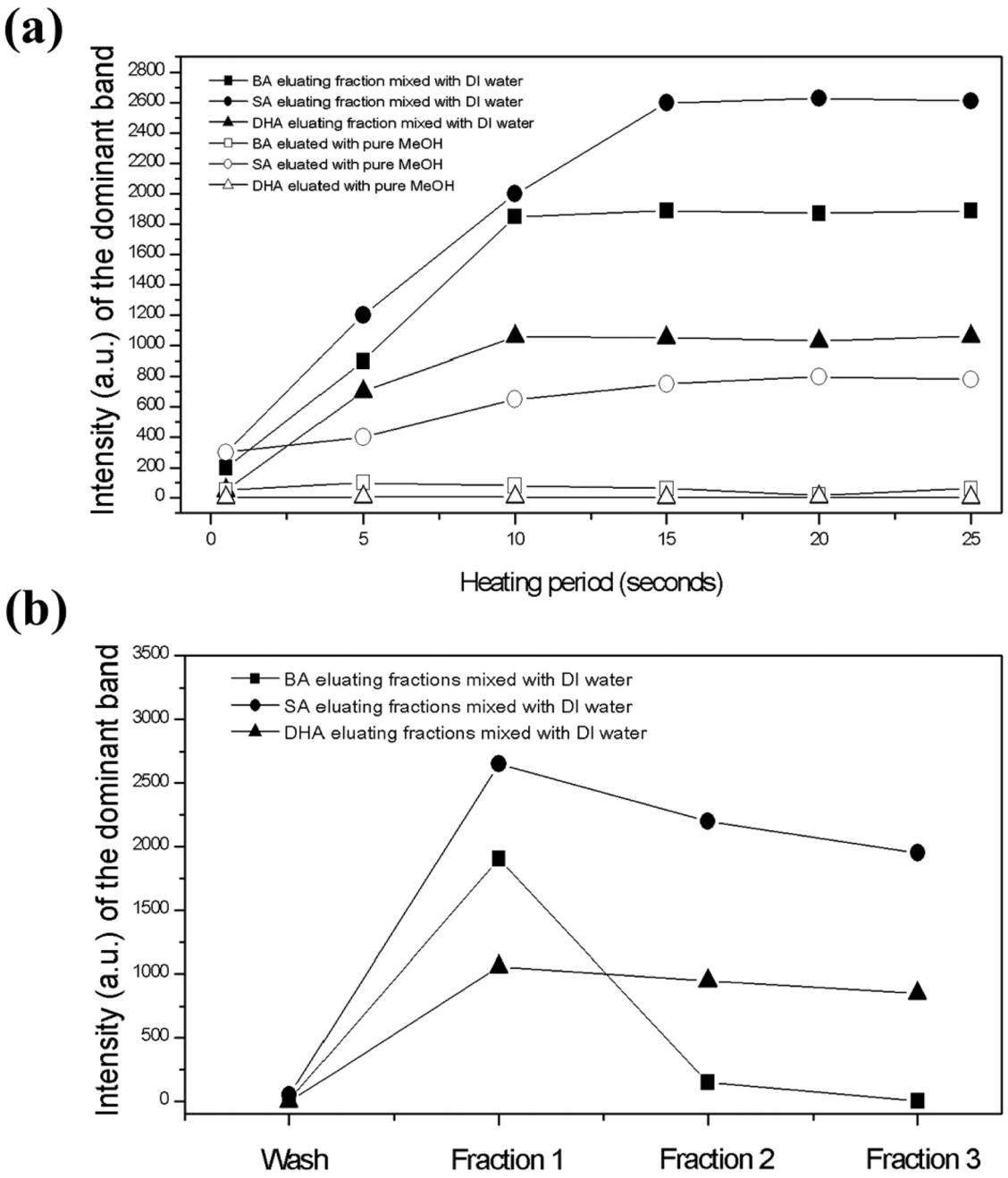

Fig. 4. (a) The intensity of the dominant bands of three preservatives, which were eluted with either a 400 μL DI water-methanol solution (2:8, V/V) or pure methanol from the SPE, varied as a function of the heating period. This period ranged from 0.5 seconds to 25 seconds. The cuttlefish ball samples were spiked with a concentration of 0.5 g/kg of BA, SA, and DHA, respectively. (b) Intensities of BA, SA, and DHA dominant bands for the first three eluting fractions. Each fraction was mixed with 200 μL DI water and deposited 4.5 μL volume onto the substrate before being heated by a 30 mW laser for 15 seconds.

was maintained at 30 mW and the volume of the drop was 4.5 μL. The SERS spectra were then acquired after the completion of the heating. The intensity of the BA-dominant band at 1002 cm^{-1} reached its maximum at 15 seconds, while the SA and DHA-dominant bands at 1645 cm^{-1} and 631 cm^{-1} reached their maximum at 10 seconds, respectively. Within the heating periods that ranged from 15 to 25 seconds, there was little variation in the intensities of the dominant bands for the three preservatives. However, when the elution solvent was substituted with pure methanol and directly deposited onto the substrate, the band intensities significantly diminished. This is probably because the recirculating twin vortices were destroyed in the methanol droplet. Furthermore, the intensities of BA, SA, and DHA dominant bands for the first three eluting fractions were measured, as shown in Fig. 4(b). Each fraction was mixed with 200 μL DI water and deposited 4.5 μL volume onto the substrate before being heated by a 30 mW laser for 15 seconds. In the first fraction, most of the BA was eluted from the cartridge. The intensity of the band, where BA is dominant, in fraction 2 was only 10 % of that in fraction 1. Similarly, the bands where SA and DHA are dominant showed their maximum intensities in fraction 1.

3.3. Detection of formulated BA, SA, and DHA preservatives in processed foods

To understand the relationship between the concentrations of the three preservatives and the intensities of the dominant Raman bands, we prepared and pretreated spiked samples with varying concentrations,

using the procedure described in Section 2.3. The first eluting fraction was mixed with 200 μL of DI water, and a droplet volume of 4.5 μL was gently deposited on the SERS substrate. The spectra were acquired with an integration time of 2 seconds and a power of 50 mW after 15 seconds of 30 mW laser heating. Fig. 5(a) and (b) illustrate the linear relationship between the logarithmic intensities and the concentrations of BA ($Log(y) = 0.9278Log(x) + 0.6985$, R^2=0.9762) and SA ($Log(y) = 0.86Log(x) + 1.1007$, R^2=0.9556) in cuttlefish ball, respectively. The dominant band of BA was 1002 cm^{-1} and that of SA was 1645 cm^{-1}. The linear relationship between the logarithmic intensities and the concentrations of DHA ($Log(y) = 0.8847Log(x) + 0.5639$, R^2=0.9817) for cheese samples is shown in Fig. 5(c). The dominant band among the Raman bands of DHA was at 631 cm^{-1}. Each data point represents an average from five samples, and each error bar indicates the standard deviation. These linear curves provided a calibration for semi-quantitative detection of the preservatives in processed foods.

Fig. 6(a) shows the measured SERS spectrum of cuttlefish ball that were spiked with 0.2 g/kg BA and 0.2 g/kg SA. The spectrum includes bands at 845 cm^{-1}, 1002 cm^{-1}, 1154 cm^{-1}, 1595 cm^{-1} and 1645 cm^{-1}, indicating that both BA and SA could be detected and identified simultaneously. The intensities of the bands at 845 cm^{-1} and 1002 cm^{-1} increased upon the addition of BA from 0.2 g/kg to 0.3 g/kg, as shown in Fig. 6(b). When the concentrations of BA and SA were increased from 0.2 g/Kg to 0.3 g/kg, the intensities of the bands at 845 cm^{-1}, 1002 cm^{-1}, 1154 cm^{-1}, 1595 cm^{-1} and 1645 cm^{-1} increased, as shown in Fig. 6(c). The limit of detection (LOD) and Limit of quantification (LOQ) were determined as follows, according to the International Union of Pure and Applied Chemistry (IUPAC) method (Long and Winefordner, 1983):

$$LOD = \frac{3S_b}{b} \quad (2)$$

$$LOQ = \frac{10S_b}{b} \quad (3)$$

where S_b is the standard deviation of the SERS intensity of the blank at the bands of 1002 cm^{-1}(BA), 1645 cm^{-1}(SA), and 631 cm^{-1} (DHA), while b represents the slope of plotted calibration curve. Fig. 6(d) and (e) show the measured spectra following the addition of 0.05 g/kg BA and 0.05 SA in cuttlefish balls, respectively. The Raman bands of BA at

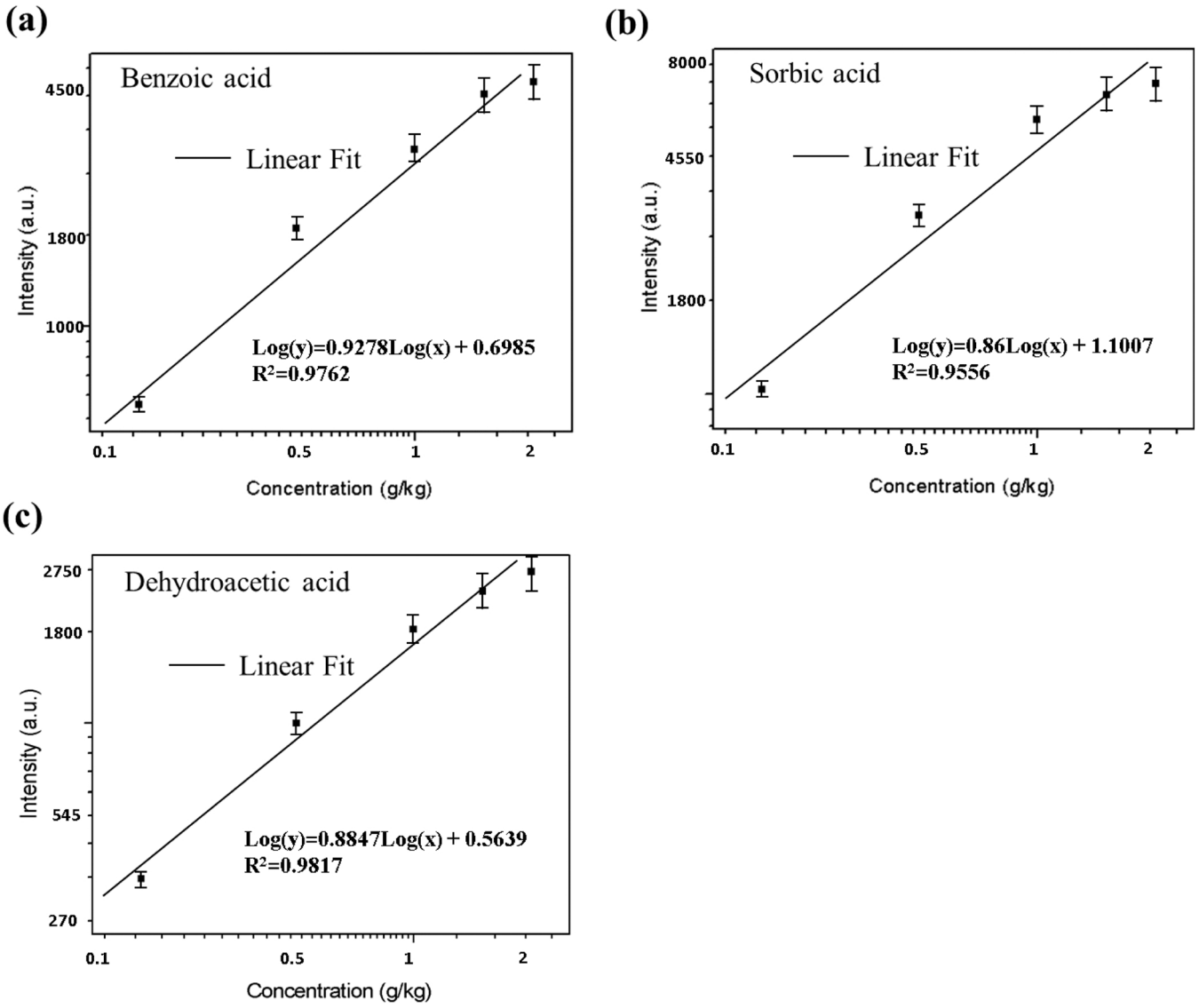

Fig. 5. The linear relationship between the logarithmic intensities of the dominant bands and the concentrations of (a) BA, (b) SA in cuttlefish ball, and (c) DHA in cheese samples. Each data point indicated an average from five samples, and each error bar indicated the standard deviation. The dominant bands of BA, SA, and DHA were 1002 cm^{-1}, 1645 cm^{-1}, and 631 cm^{-1}, respectively.

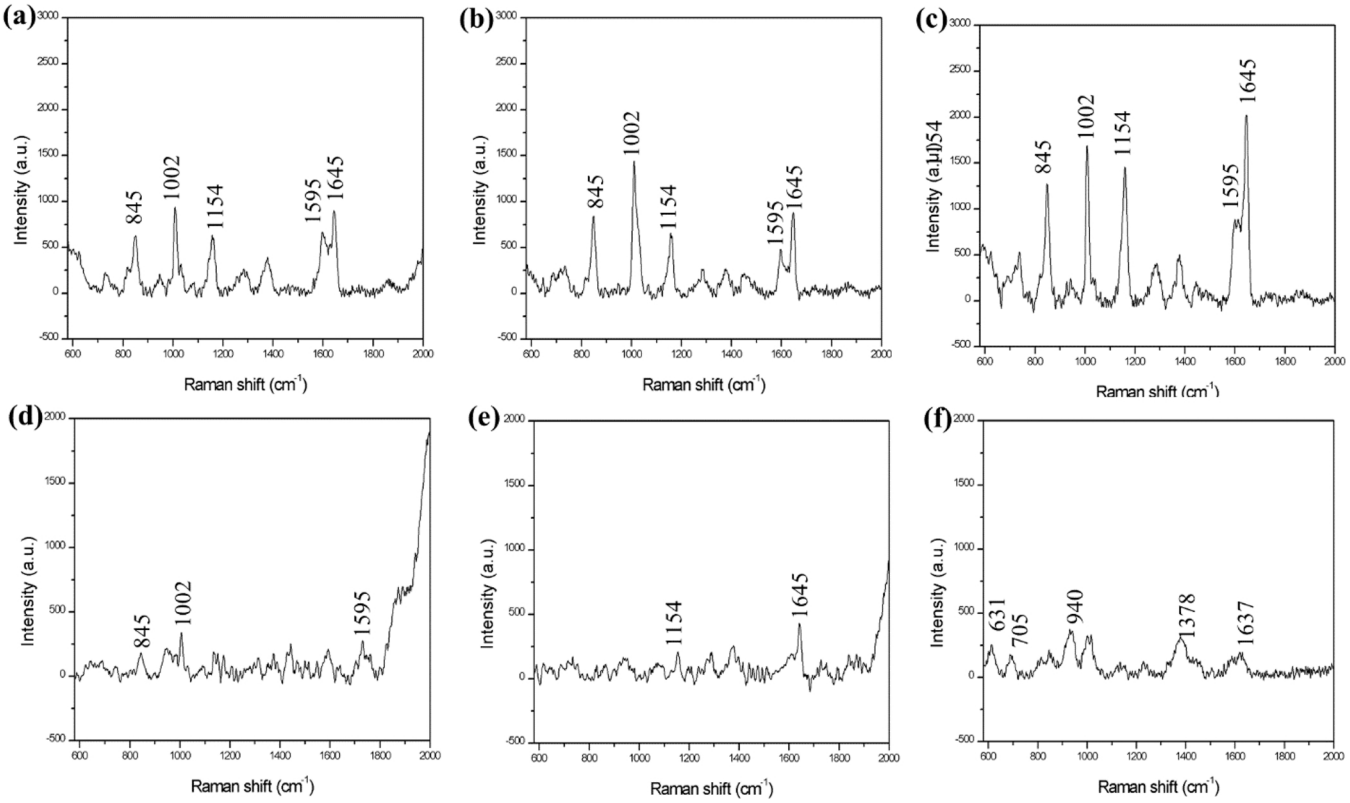

Fig. 6. (a) SERS spectrum of cuttlefish balls with added 0.2 g/kg BA and 0.2 g/kg SA. (b) SERS spectrum of cuttlefish balls with added 0.3 g/kg BA and 0.2 g/kg SA. (c) SERS spectrum of cuttlefish balls with added 0.3 g/kg BA and 0.3 g/kg SA. SERS spectrum following addition of (d) 0.05 g/kg BA, (e) 0.05 g/kg SA in cuttlefish ball, and (f) 0.10 g/kg DHA in cheese sample.

845 cm^{-1}, 1002 cm^{-1} and 1595 cm^{-1}, and the Raman bands of SA at 1154 cm^{-1} and 1645 cm^{-1}, were observed. Fig. 6(f) shows the measured spectra following the addition of 0.10 g/kg DHA spiked in cheese sample. The Raman bands at 631 cm^{-1}, 705 cm^{-1}, 940 cm^{-1}, and 1595 cm^{-1} were observed. From these results, the signal-to-noise (S/N) ratios of 3.62, 4.14, and 3.25 for BA, SA, and DHA were obtained, respectively. Therefore, the LODs for BA and SA were measured to be as low as 0.05 g/kg, and the LOD for DHA was found to be as low as 0.10 g/kg. The LOQs were then calculated to be 0.183 g/kg, 0.144 g/kg, and 0.201 g/kg for BA, SA, and DHA, respectively. Furthermore, based on the evaluation of the human health impact of each preservative, the FDA in each country establishes the MRLs for each preservative in various processed foods. The Taiwan Food and Drug Administration (TFDA) has set an MRL for processed minced fish and seafood products at 2.0 g/kg for SA and 1.0 g/kg for BA, respectively. The combined amount of SA and BA should not exceed 1.0 g/kg. The MRLs for cheese have been set at 1.0 g/kg for SA and 0.5 g/kg for DHA, respectively. Compared with the MRLs, the LODs of the three preservatives could meet this requirement.

3.4. Determination of screening efficiency in real samples

To verify the practical applications of the presented detection method, we analyzed 30 samples of processed minced fish and seafood products, along with 20 cheese samples, all of which had been purchased from a supermarket. All processed samples were placed into clean plastic bags and frozen at −18 °C ± 2 °C overnight. The following day, the required amounts of frozen samples were removed and comminuted thoroughly to achieve the best sample homogeneity. A 2 g (± 0.1 g) amount of previously homogenized sample was placed into a 15 mL centrifuge tube. Five mL DI water-methanol solution (1:1, V/V, DI H_2O/MeOH) was added to each tube using the dispenser. The tubes were capped, vortexed for 1 minute, and then left to sit for 3 minutes. Prior to the use of the PT-001 SPE cartridge, a 2 mL DI water-methanol solution (1:1, V/V, DI H2O/MeOH) was passed through the cartridge as a conditioning solvent. A 200 μL volume of the supernatant was then loaded and passed through the SPE cartridge. Following that, the cartridge was washed with 600 μL DI water-methanol solution (8:2, V/V, DI H_2O/MeOH) at a flow rate of one drip per second to remove impurities. The preservatives BA, SA, and DHA were eluted with a 400 μL DI water-methanol solution (2:8, V/V, DI H_2O/MeOH) at a flow rate of one drip per second. Next, the eluting fraction was mixed with 200 μL of DI water, and a droplet volume of 4.5 μL was gently deposited on the substrate. After 15 seconds of 30 mW laser heating at the center of the droplet, the spectra of the food samples were obtained using a portable Raman spectrometer (RMS-1000) with a 785 nm laser source. The resolution of the spectrometer was 12 cm^{-1} and the focal length of the objective was 7.5 mm±0.5 mm. Instrument parameters were set as follows: integration time of 2 seconds and 50 mW laser power.

To evaluate the screening efficiency of the detection method, the amounts of the preservatives in the samples were determined by the standard method (MOHWA0020.03) for analyzing preservatives in foods as specified by the TFDA. The LOD and the limit of quantification (LOQ) of the standard method were 0.0001 g/kg and 0.02 g/kg (Agilent 1200 series HPLC coupled with Agilent 6410 Triple Quadruple LC/MS), respectively. Table A.1 presents the liquid chromatography and tandem mass spectrometer condition.

As shown in Table 1, 30 samples of processed minced fish and seafood products were measured and analyzed for BA and SA. Eight samples tested positive for SA and only one contained the minimal BA concentration of 0.002 g/kg. Sample 28 contained the highest concentration of SA, which was 1.387 g/kg, and it yielded the most intense 1645 cm^{-1} band. The measured spectra of the 30 samples were shown in Fig. 7. The Raman bands of 1154 and 1645 cm^{-1} for SA were identified in several

Table 1
Amounts of BA an SA added to samples determined using MOHWA0020.03 method and SERS.

Sample	Food type	MOHWA0020.03[a]		SERS					
		BA Detected (g/kg)	SA Detected (g/kg)	Peaks found (cm^{-1})	BA Intensity[f] (a.u.)	Detected[d] (g/kg)	Peaks found (cm^{-1})	SA Intensity[g] (a.u.)	Detected[d] (g/kg)
1	cuttlefish ball	N.D.[c]	N.D.[c]	-	-	N.D.[e]	-	-	N.D.[e]
2	cuttlefish ball	N.D.	N.D.	-	-	N.D.	-	-	N.D.
3	cuttlefish shrimp ball	N.D.	N.D.	-	-	N.D.	-	-	N.D.
4	sailfish ball	N.D.	N.D.	-	-	N.D.	-	-	N.D.
5	milkfish ball	N.D.	N.D.	-	-	N.D.	-	-	N.D.
6	salmon ball	N.D.	N.D.	-	-	N.D.	-	-	N.D.
7	kamaboko	N.D.	0.443	-	-	N.D.	1154、1645	3380	0.666
8	cuttlefish ball	N.D.	N.D.	-	-	N.D.	-	-	N.D.
9	kamaboko	N.D.	0.012	-	-	N.D.	1154、1645	250	<LOQ[h]
10	caviar ball	N.D.	N.D.	-	-	N.D.	-	-	N.D.
11	shrimp dumpling	N.D.	N.D.	-	-	N.D.	-	-	N.D.
12	cuttlefish dumpling	N.D.	N.D.	-	-	N.D.	-	-	N.D.
13	fish dumpling	N.D.	N.D.	-	-	N.D.	-	-	N.D.
14	squid paste	N.D.	N.D.	-	-	N.D.	-	-	N.D.
15	cod ball	N.D.	N.D.	-	-	N.D.	-	-	N.D.
16	tempura	N.D.	N.D.	-	-	N.D.	-	-	N.D.
17	fish ball	N.D.	N.D.	-	-	N.D.	-	-	N.D.
18	milkfish ball	N.D.	0.560	-	-	N.D.	1154、1645	4350	0.893
19	tempura	N.D.	0.922	-	-	N.D.	1154、1645	5201	1.099
20	shrimp ball	0.002[b]	N.D.	1002	95	< LOD[d]	-	-	N.D.
21	kamaboko	N.D.	0.806	-	-	N.D.	1154、1645	4962	1.040
22	crab stick	N.D.	N.D.	-	-	N.D.	-	-	N.D.
23	octopus kamaboko	N.D.	0.820	-	-	N.D.	1154、1645	5304	1.124
24	fish roe roll	N.D.	N.D.	-	-	N.D.	-	-	N.D.
25	fish paste	N.D.	0.527	-	-	N.D.	1154、1645	4241	0.867
26	squid ball	N.D.	N.D.	-	-	N.D.	-	-	N.D.
27	fish dumpling	N.D.	N.D.	-	-	N.D.	-	-	N.D.
28	tempura	N.D.	1.387	-	-	N.D.	1154、1645	6852	1.514
29	crab stick	N.D.	N.D.	-	-	N.D.	-	-	N.D.
30	fish paste	N.D.	N.D.	-	-	N.D.	-	-	N.D.

[a] HPLC: Agilent 1200, MS/MS: Agilent 6410.
[b] LOD: 0.0001 g/kg; LOQ: 0.02 g/kg.
[c] N.D.: < LOD (0.0001 g/kg).
[d] LOD (SERS): BA:0.05 g/kg、SA:0.05 g/kg.
[e] N.D.: < LOD (SERS).
[f] The major peak of BA is located at 1002 cm^{-1}.
[g] The major peak of SA is located at 1645 cm^{-1}.
[h] LOQ (SERS): BA:0.183 g/kg、 SA:0.144 g/kg

samples. From sample 9, the intensities of the SA Raman bands were weak. From sample 20, the Raman bands at 845 cm^{-1} and 1595 cm^{-1} were not observed due to the low concentration of BA. Only one band of BA with minimal intensities at 1002 cm^{-1} was obtained. Furthermore, 20 cheese samples were measured for BA, SA, and DHA and summarized in Table 2. The measured spectra of the 20 samples were shown in Fig. 8. Six samples tested positive for SA and there was no BA and DHA found in other samples. The specificity, sensitivity, false positive rate, and false negative rate were calculated as follows, to assess the screening efficiency of the detection method:

$$Specificity = \frac{TN}{TN + FP} \tag{4}$$

$$Sensitivity = \frac{TP}{TP + FN} \tag{5}$$

$$False\ positive\ rate = \frac{FP}{FP + TN} \tag{6}$$

$$False\ negative\ rate = \frac{FN}{FN + TP} \tag{7}$$

where *TP*, *FP*, *FN*, *TN* denotes the factors of screening efficiency: true positive, false negative, false positive, and true negative for sample status, respectively. Table A.2 shows the factors of screening efficiency of the method for the minced fish and seafood products, The values of specificity, sensitivity, false positive rate and false negative rate were calculated to be 100 %, 88.88 %, 0 % and 11.11 %, respectively. Table A.3 shows the factors of screening efficiency for the cheese samples. The values of specificity, sensitivity, false positive rate and false negative rate were calculated to be 100 %, 100 %, 0 % and 0 %, respectively.

Table 3 comprehensively summarizes the research progress of various detection methods for analyzing food preservatives. The microfluidic detection platform (Wu et al., 2020), incorporating an integrated reaction chip and a micro-spectrometer, was introduced to detect the absorbance spectra of BA and SA under illumination at wavelengths of 530 nm and 550 nm, respectively. The practical feasibility of the presented platform has been demonstrated by measuring processed samples with BA concentrations ranging from 0.05 to 0.5 g/kg and SA concentrations ranging from 0.02 to 0.5 g/kg. However, when both BA and SA are present in the food sample, the broad absorbance bands caused by BA and SA interfere with each other, making quantitative analysis difficult. Furthermore, a SERS-based method (Lin et al., 2020) was developed for detecting the BA content in pickled vegetables. Despite the method having a sensitivity of 100 % and a specificity of 90.9 %, it exhibited a narrow linear range from 0.38 to 0.82 g/kg between the Raman band intensity and the concentrations of BA. The LOD was 0.08 g/kg, and the LOQ was 0.265 g/kg, both of which are higher than those of the detection method proposed in this study. The SERS-related research (Yang et al., 2022; Hussain et al., 2020; Cai et al., 2018; Chien et al., 2023) provides rapid and sensitive methods for

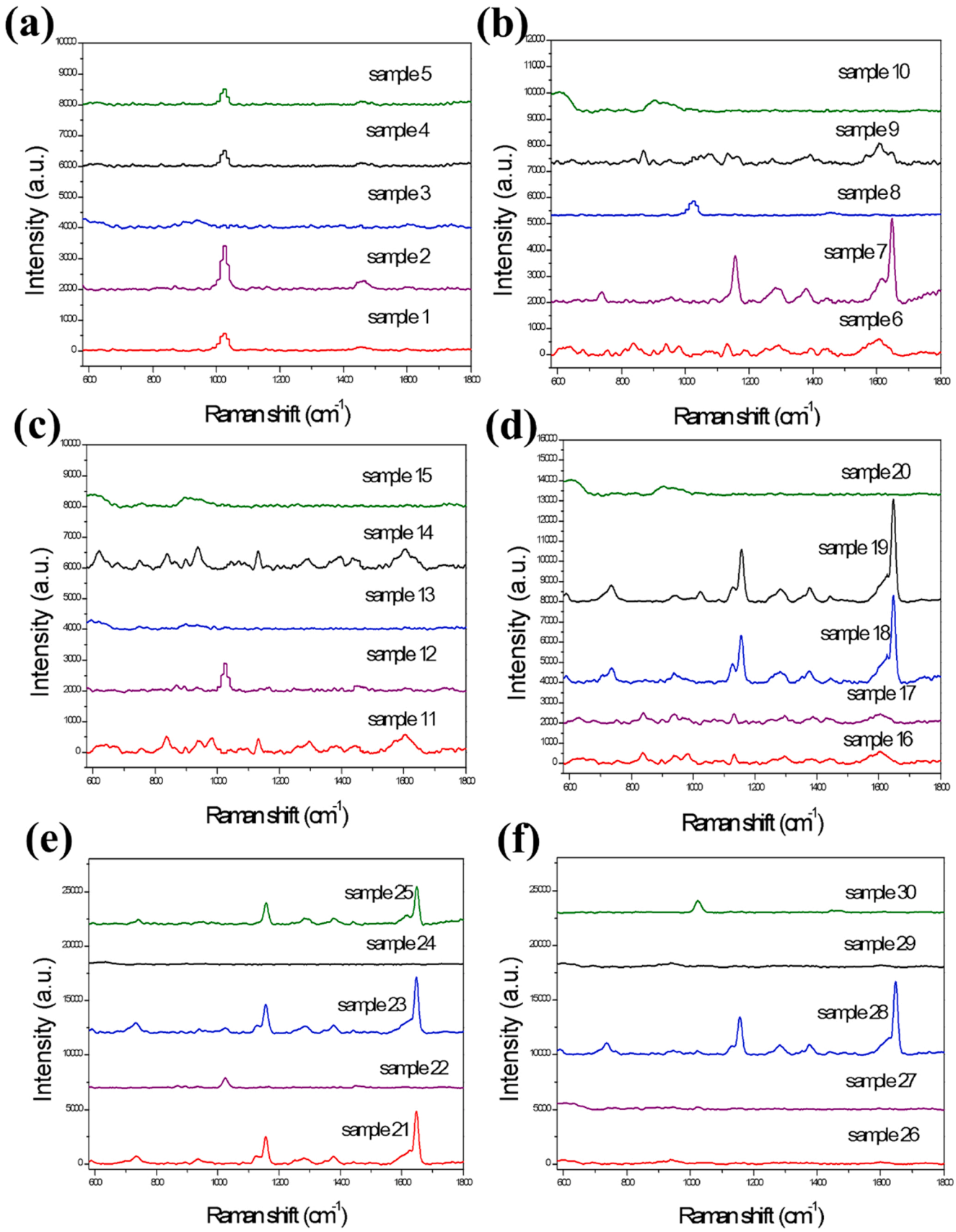

Fig. 7. SERS spectra of processed minced fish and seafood products for (a) samples 1–5, (b) samples 6–10, (c) samples 11–15, (d) samples 16–20, (e) samples 21–25 and (f) samples 26–30. The measurements were taken at an excitation wavelength of 785 nm, with an acquisition time of 2 seconds and a laser power of 50 mW.

Table 2
Amounts of BA, SA and DHA added to cheese samples determined using MOHWA0020.03 method and SERS.

Sample	Food type	MOHWA0020.03[a]			SERS								
		BA Detected (g/kg)	SA Detected (g/kg)	DHA Detected (g/kg)	Peaks found (cm^{-1})	BA Intensity (a.u.)[f]	Detected (g/kg)[d]	Peaks found (cm^{-1})	SA Intensity (a.u.)[g]	Detected (g/kg)[d]	Peaks found (cm^{-1})	DHA Intensity (a.u.)[h]	Detected (g/kg)[d]
1	Cheddar cheese	N.D.[b,c]	N.D.[b,c]	N.D.[b,c]	-	-	N.D.[e]	-	-	N.D.[e]	-	-	N.D.[e]
2	Gouda cheese	N.D.	0.134	N.D.	-	-	N.D.	**1154、1645**	589	< LOQ[i]	-	-	N.D.
3	Processed cheese	N.D.	0.159	N.D.	-	-	N.D.	**1154、1645**	744	0.114	-	-	N.D.
4	Sweet potato cheese	N.D.	N.D.	N.D.	-	-	N.D.	-	-	N.D.	-	-	N.D.
5	Mozzarella cheese	N.D.	N.D.	N.D.	-	-	N.D.	-	-	N.D.	-	-	N.D.
6	Processed cheese	N.D.	N.D.	N.D.	-	-	N.D.	-	-	N.D.	-	-	N.D.
7	Cheddar cheese	N.D.	0.166	N.D.	-	-	N.D.	**1154、1645**	817	0.127	-	-	N.D.
8	Mozzarella cheese	N.D.	N.D.	N.D.	-	-	N.D.	-	-	N.D.	-	-	N.D.
9	Cheddar cheese	N.D.	N.D.	N.D.	-	-	N.D.	-	-	N.D.	-	-	N.D.
10	Processed cheese	N.D.	N.D.	N.D.	-	-	N.D.	-	-	N.D.	-	-	N.D.
11	Processed cheese	N.D.	0.115	N.D.	-	-	N.D.	**1154、1645**	621	< LOQ[i]	-	-	N.D.
12	Processed cheese	N.D.	N.D.	N.D.	-	-	N.D.	-	-	N.D.	-	-	N.D.
13	Processed cheese	N.D.	N.D.	N.D.	-	-	N.D.	-	-	N.D.	-	-	N.D.
14	Parmesan cheese	N.D.	0.221	N.D.	-	-	N.D.	**1154、1645**	1050	0.171	-	-	N.D.
15	Truffle cheese	N.D.	N.D.	N.D.	-	-	N.D.	-	-	N.D.	-	-	N.D.
16	Processed cheese	N.D.	N.D.	N.D.	-	-	N.D.	-	-	N.D.	-	-	N.D.
17	Mozzarella cheese	N.D.	N.D.	N.D.	-	-	N.D.	-	-	N.D.	-	-	N.D.
18	Mozzarella cheese	N.D.	N.D.	N.D.	-	-	N.D.	-	-	N.D.	-	-	N.D.
19	Emmental cheese	N.D.	0.203	N.D.	-	-	N.D.	**1154、1645**	981	0.158	-	-	N.D.
20	Processed cheese	N.D.	N.D.	N.D.	-	-	N.D.	-	-	N.D.	-	-	N.D.

[a] HPLC: Agilent 1200, MS/MS: Agilent 6410.
[b] LOD: 0.0001 g/kg; LOQ: 0.02 g/kg.
[c] N.D.: < LOD (0.0001 g/kg).
[d] LOD (SERS): BA: 0.05 g/kg、SA: 0.05 g/kg、DHA: 0.10 g/Kg
[e] N.D.: < LOD (SERS)
[f] The major peak of BA is located at 1002 cm^{-1}.
[g] The major peak of SA is located at 1645 cm^{-1}.
[h] The major peak of DHA is located at 631 cm^{-1}.
[i] LOQ (SERS): BA:0.183 g/kg、SA:0.144 g/kg、DHA: 0.201 g/kg.

determining BA content in liquid milk, carbonated beverages, and electronic cigarette liquids. Without sample pretreatment (Chien et al., 2023), part of the SERS signal of BA was suppressed due to the interference of fluorescence background. Two Raman bands of BA at 845 cm^{-1} and 1595 cm^{-1} vanished, and only the BA-dominant band at 1002 cm^{-1} was observed. Consequently, the method presented both a false negative rate of 4.4 % and a false positive rate of 8.9 % after examining 406 commercial e-liquids. Moreover, the absolute quantification method for detecting three kinds of preservatives (BA, SA, and DHA) in processed foods using quantitative ^{1}H nuclear magnetic resonance spectroscopy (qHNMR) was developed (Ohtsuki et al., 2012a, 2012b, Ohtsuki et al., 2013). The accuracy of the method is equivalent to the conventional method using HPLC, but it requires laboratory-equipped instruments and skilled personnel. Another sensitive method for quantitative determination of BA and SA in soy sauces (Wei et al., 2011) was introduced using field-amplified sample injection with capacitively coupled contactless conductivity detection (FESI-CE-C^4D). However, the FESI-CE-C^4D method requires 85 minutes for sample preparation and 15 minutes for analysis, including the determination of preservatives. The time-consuming sample pretreatment of the method needs a stream of nitrogen gas to evaporate the organic phase solution in the laboratory environment, which is difficult to conduct for on-site quality control in restaurants and supermarkets. In contrast, the SERS method proposed in this study provides a rapid approach for simultaneously detecting added BA, SA, and DHA in processed foods. The sample pretreatment was simplified, and the extracts were processed using the PT-001 SPE within 10 minutes. Notably, local heating at the center of the droplet deposited onto the SERS substrate was introduced to increase the binding probability between the molecules and the metallic surface, resulting in an increase in the Raman

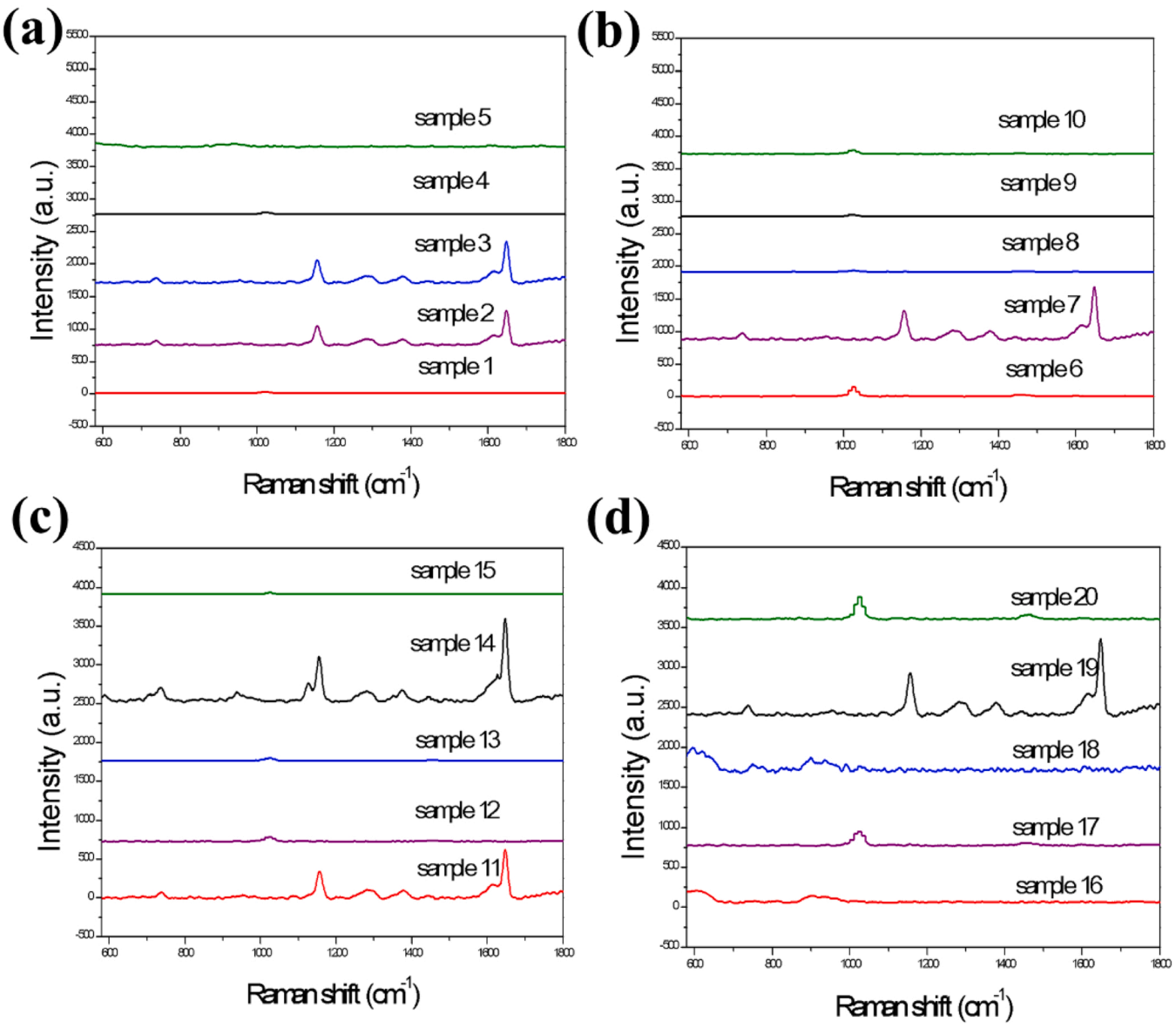

Fig. 8. SERS spectra of cheese products for (a) samples 1–5, (b) samples 6–10, (c) samples 11–15, (d) samples 16–20. The measurements were taken at an excitation wavelength of 785 nm, with an acquisition time of 2 seconds and a laser power of 50 mW.

signals of the preservatives and excellent screening efficiency in real samples.

4. Conclusion

A rapid method for simultaneously detecting added BA, SA, and DHA in processed foods was developed based on SERS and SPE techniques. The dominant bands of BA, SA, and DHA were measured and identified to be 1002 cm^{-1}, 1645 cm^{-1}, and 631 cm^{-1} at a wavelength of 785 nm, respectively. The sample pretreatment was simplified and the extracts were processed using the PT-001 SPE within 10 minutes, following the load, wash and elution steps. A droplet from the first eluting fraction was mixed with 200 μL DI water and gently deposited onto a substrate of silver nanopillar arrays with 2.2 mm × 2.2 mm area. Local heating was then applied at the center of the substrate using a 30 mW CW laser for a duration of 15 seconds. After the heating, the SERS spectra were acquired with an integration time of 2 seconds and a power of 50 mW using a portable Raman spectrometer. A droplet of 4.5 μL was found to have a contact angle of 89° between the drop and the substrate. This was determined to be the optimized volume to induce the merging of twin vortices within the droplet, resulting in the strongest SERS signal of the preservatives. Furthermore, the intensities of BA, SA, and DHA dominant Raman bands with different heating periods that ranged from 15 to 25 seconds were measured. The intensity of the BA-dominant band at 1002 cm^{-1} reached its maximum at 15 seconds, while the SA and DHA-dominant bands at 1645 cm^{-1} and 631 cm^{-1} reached their maximum at 10 seconds, respectively. Moreover, the linear relationship between the logarithmic intensities of the dominant bands and the concentrations of BA, SA, and DHA in processed foods were established. The LOD for both BA and SA was experimentally determined to be as low as 0.05 g/kg, while the LOD for DHA was 0.1 g/kg. The linear curves provided a calibration for semi-quantitative detection of the preservatives in processed foods. The screening efficiency of the detection method for the preservatives was experimentally evaluated in real samples, such as processed seafood, minced fish, and cheese products. The band intensities of the added preservatives were compared with amounts obtained by the conventional method of HPLC. Consequently, the rapid method for the simultaneous detection of BA, SA, and DHA in processed foods was proposed and demonstrated for the first time using SERS. It can be extended to the detection of parabens in the future, such as

Table 3
Comprehensively summarizes the research progress of various detection methods for analyzing food preservatives.

Detection method	Target	Sample type	Total detection time	Linear range	LOD	LOQ	Screening efficiency	Reference
SERS	BA SA DHA	processed foods	15 minutes	0.183 – 2 g/kg (BA) 0.144 – 2 g/kg (SA) 0.201 – 2 g/kg (DHA)	0.05 g/kg (BA) 0.05 g/kg (SA) 0.10 g/kg (DHA)	0.183 g/kg (BA) 0.144 g/kg (SA) 0.201 g/kg (DHA)	processed foods/ cheese: Specificity: 100 %、100 % Sensitivity: 88.88 %、100 % false positive rate: 0 、0 % false negative rate: 11.11 % 、0 %	**This study**
SERS	BA	pickled vegetables	25 minutes	0.38–0.82 g/kg	0.08 g/kg	0.265 g/kg	Specificity: 100 % Sensitivity: 90.9 % false positive rate: 9.1 % false negative rate: 0 %	(Lin et al., 2020)
Microfluidic analysis platform with micro-distillation extraction	BA SA	processed foods	49 minutes	0.05 – 2.0 g/kg (BA) 0.02 – 0.5 g/kg (SA)	not shown	not shown	not shown	(Wu et al., 2020)
Quantitative^{1}H nuclear magnetic resonance spectroscopy(qHNMR) with solvent extraction	BA	processed foods	55 minutes	0.063–5.0 g/kg	not shown	0.063 g/kg	not shown	(Ohtsuki et al., 2012a)
	SA		55 minutes	0.063–5.0 g/kg	not shown	0.063 g/kg	not shown	(Ohtsuki et al., 2012b)
	DHA		65 minutes	0.13–5.0 g/kg	not shown	0.13 g/kg	not shown	(Ohtsuki et al., 2013)
SERS	BA	liquid milk	15 minutes	2–20 μg/mL	0.13 μg/mL	2 μg/mL	not shown	(Yang et al., 2022)
SERS	BA	liquid milk	12 minutes	10.2–240 μg/mL	9.8 μg/mL	10.2 μg/mL	not shown	(Hussain et al., 2020)
SERS	BA	carbonated beverages	25 minutes	25–500 μg/mL	3.6 μg/mL	25 μg/mL	not shown	(Cai et al., 2018)
SERS	BA	electronic cigarette liquids	5 minutes	not shown	not shown	not shown	Sensitivity: 90 % false positive rate: 2.5–4.4 % false negative rate: 4.4–8.9 %	(Chien et al., 2023)
Field-amplified sample injection with capacitively coupled contactless conductivity detection (FESI-CE-C^{4}D)	BA SA	soy sauce	100 minutes	0.3–20.0 μM (BA) 0.3–20.0 μM (SA)	0.08 μM (BA) 0.05 μM (SA)	0.3 μM	not shown	(Wei et al., 2011)

methylp-hydroxybenzoate (methylparaben), ethylp-hydroxybenzoate (ethylparaben), and propyl p-hydroxybenzoate (propylparaben).

Abbreviations

GLAD: Glancing Angle Deposition; SERS: Surface Enhanced Raman Scattering; SPE: Solid-Phase Extraction; AEF: Analytical Enhancement Factor; BA: Benzoic Acid; SA: Sorbic Acid; EEM: Electromagnetic Enhancement Mechanism; DHA: Dehydroacetic Acid; MRLs: Maximum Residue Limits; LOD: Limit Of Detection; LOQ: Limit of Quantification; HPLC: High-Performance Liquid Chromatograph.

Ethical approval

This article does not contain any studies with human participants or animals performed by any of the authors.

CRediT authorship contribution statement

Sz-Ying Chen: Formal analysis, Data curation. **Zi-Ting Yang:** Formal analysis, Data curation. **Chao-Ming Tsen:** Writing – review & editing, Validation, Formal analysis. **Ching-Wei Yu:** Writing – original draft, Methodology. **Yi-Jun Jen:** Writing – review & editing, Supervision, Conceptualization.

Declaration of Competing Interest

The authors declare that they have no known competing financial interests or personal relationships that could have appeared to influence the work reported in this paper.

Data availability

Data will be made available on request.

Acknowledgements

This work was supported by the National Science and Technology Council of the Republic of China, Taiwan [MOST 111–2221-E-027–038-MY3]; the Ministry of Agriculture of the Republic of China, Taiwan [113AS-13.1.1-PI-01].

Informed consent

Not applicable

Appendix A. Supporting information

Supplementary data associated with this article can be found in the online version at doi:10.1016/j.jfca.2024.106740.

References

Alagöz, S., Türkyılmaz, M., Tağı, Ş., Özkan, M., 2015. Effects of different sorbic acid and moisture levels on chemical and microbial qualities of sun-dried apricots during storage. Food Chem. 174, 356–364. https://doi.org/10.1016/j.foodchem.2014.11.075.

Amirpour, M., Arman, A., Yolmeh, A., Azam, M.A., Moradi-Khatoonabadi, Z., 2015. Sodium benzoate and potassium sorbate preservatives in food stuffs in Iran. Food Addit. Contam.: Part B 8 (2), 142–148. https://doi.org/10.1080/19393210.2015.1021862.

Askounis, A., Kita, Y., Kohno, M., Takata, Y., Koutsos, V., Sefiane, K., 2017. Influence of local heating on Marangoni flows and evaporation kinetics of pure water drops. Langmuir 33 (23), 5666–5674. https://doi.org/10.1021/acs.langmuir.7b00957.

Aubourg, S.P., Medina, I., 1997. Quality differences assessment in canned sardine (Sardina pilchardus) by fluorescence detection. J. Agric. Food Chem. 45, 3617–3621. https://doi.org/10.1021/jf970056l.

Aubourg, S.P., Medina, I., Gallardo, J.M., 1998. Quality assessment of blue whiting (micromesistius poutassou) during chilled storage by monitoring lipid damages. J. Agric. Food Chem. 46, 3662–3666. https://doi.org/10.1021/jf980362e.

Billes, F., Elečková, L., Mikosch, H., Andruch, V., 2015. Vibrational spectroscopic study of dehydroacetic acid and its cinnamoyl pyrone derivatives. Spectrochim. Acta Part A: Mol. Biomol. Spectrosc. 146, 97–112. https://doi.org/10.1016/j.saa.2015.03.010.

Cai, L., Dong, J., Wang, Y., Chen, X., 2018. Thin-film microextraction coupled to surface enhanced Raman scattering for the rapid detection of benzoic acid in carbonated beverages. Talanta 178, 268–273. https://doi.org/10.1016/j.talanta.2017.09.040.

Cai, C., Zhou, F., Chu, R., Ye, H., Zhang, C., Shui, L., Liu, Ye, 2024. Rapid and sensitive in-situ detection of pesticide residues in real tea soup with optical fiber SERS probes. J. Food Compos. Anal. 134, 106520 https://doi.org/10.1016/j.jfca.2024.106520.

Chien, J.-Y., Gu, Y.-C., Liu, C.-H., Tsai, H.-M., Lee, C.-N., Yang, A.C., Huang, J., Wang, Y.-L., Wang, J.-K., Lin, C.-H., 2023. Rapid detection of nicotine and benzoic acid in e-liquids with surface-enhanced Raman scattering and artificial intelligence-assisted spectrum interpretation. J. Pharm. Biomed. Anal. 233, 115456 https://doi.org/10.1016/j.jpba.2023.115456.

Choi, S.-H., Park, H.G., 2005. Surface-enhanced Raman scattering (SERS) spectra of sodium benzoate and 4-picoline in Ag colloids prepared by g-irradiation. Appl. Surf. Sci. 243, 76–81. https://doi.org/10.1016/j.apsusc.2004.09.051.

Chu, H.Y., Liu, Y., Huang, Y., Zhao, Y., 2007. A high sensitive fiber SERS probe based on silver nanorod arrays. Opt. Express 15, 12239. https://doi.org/10.1364/OE.15.012230.

Diddens, C., Li, Y., Lohse, D., 2021. Competing Marangoni and Rayleigh convection in evaporating binary droplets. J. Fluid Mech. 914, A23 https://doi.org/10.1017/jfm.2020.734.

Dong, C., Wang, W., 2006. Headspace solid-phase microextraction applied to the simultaneous determination of sorbic and benzoic acids in beverages. Anal. Chim. Acta 562, 23–29. https://doi.org/10.1016/j.aca.2006.01.045.

Fang, B., Xu, S., Huang, Y., Su, F., Huang, Z., Fang, H., Peng, J., Xiong, Y., Lai, W., 2020. Gold nanorods etching-based plasmonic immunoassay for qualitative and quantitative detection of aflatoxin M1 in milk. Food Chem. 329, 127160 https://doi.org/10.1016/j.foodchem.2020.127160.

Feng, Z., Zhang, P., Yang, X., Guo, X., Yu, J., Du, L., Shao, J., Liang, H., Jiang, H., 2024. Simultaneous detection of two pesticide residues in tobacco leaves using SiO2@Ag-SERS substrate and portable Raman spectrometer. J. Food Compos. Anal. 133, 106461 https://doi.org/10.1016/j.jfca.2024.106461.

Gao, J., Hu, Y., Li, S., Zhang, Y., Chen, X., 2013. Adsorption of benzoic acid, phthalic acid on gold substrates studied by surface-enhanced Raman scattering spectroscopy and density functional theory calculations. Spectrochim. Acta, Part A: Mol. Biomol. Spectrosc. 104, 41–47. https://doi.org/10.1016/j.saa.2012.11.103.

Hassoun, A., Sahar, A., Lakhal, L., Aït-Kaddour, A., 2019. Fluorescence spectroscopy as a rapid and non-destructive method for monitoring quality and authenticity of fish and meat products: Impact of different preservation conditions. LWT-Food Sci. Technol. 103, 279–292. https://doi.org/10.1016/j.lwt.2019.01.021.

Hussain, A., Pu, H., Sun, D.-W., 2020. SERS detection of sodium thiocyanate and benzoic acid preservatives in liquid milk using cysteamine functionalized core-shelled nanoparticles. Spectrochim. Acta, Part A: Mol. Biomol. Spectrosc. 229, 117994 https://doi.org/10.1016/j.saa.2019.117994.

Jen, Y.-J., Chan, S., Huang, Jheng, J.-W., C.-Y, Liu, W.-C., 2010. Self-shadowing deposited pure metal nanohelix arrays and SERS application. Nanoscale Res. Lett. 10, 498. https://doi.org/10.1186/s11671-015-1205-8.

Jen, Y.-J., Huang, J.-W., Liu, Chan, W.-C.S., Tseng, C.-H., 2016. Glancing angle deposited gold nanohelix arrays on smooth glass as three-dimensional SERS substrates. Opt. Mater. Express 6, 697–704. https://doi.org/10.1364/OME.6.000697.

Jen, Y.J., Lin, M.J., Cheang, H.L., Chan, T.L., 2019. Obliquely deposited titanium nitride nanorod arrays as surface-enhanced Raman scattering substrates. Sensors 19, 4765. https://doi.org/10.3390/s19214765.

Jen, Y.-J., Liu, W.-C., Cong, Chan, M.-Y., T.-L, 2020. Bideposited silver nanocolloid arrays with strong plasmon-induced birefringence for SERS application. Sci. Rep. 10, 20143 https://doi.org/10.1038/s41598-020-77149-0.

Jen, Y.-J., Suzuki, M., Wang, Y.-H., Lin, M.-J., 2012. Near-field simulation of obliquely deposited surface-enhanced Raman scattering substrates. J. Appl. Phys. 112, 113111 https://doi.org/10.1063/1.4769806.

Kai, S., Chaozhi, W., Guangzhi, X., 1989. Multiple adsorbed states and surface enhanced Raman spectra of crotonic and sorbic acids on silver hydrosols. J. Raman Spectrosc. 20, 267–271. https://doi.org/10.1002/jrs.1250200412.

Kumar, S., Gahlaut, K.S., Singh, J.P., 2022. Sculptured thin films: overcoming the limitations of surface-enhanced Raman scattering substrates. Appl. Surf. Sci. Adv. 12, 100322 https://doi.org/10.1016/j.apsadv.2022.100322.

Kumar, S., Tokunaga, K., Namura, K., Fukuoka, T., Suzuki, M., 2020. Experimental evidence of a twofold electromagnetic enhancement mechanism of surface-enhanced Raman scattering. J. Phys. Chem. C. 124 (38), 21215–21222. https://doi.org/10.1021/acs.jpcc.0c07930.

Lei, C., Wei, C., Chen, M., Ou, S., Li, W.-H., Lee, K.C., 1995. Enhanced Raman scattering from crystal violet and benzoic acid molecules adsorbed on silver nanocrystals. Mater. Sci. Eng.: B 32, 39–45. https://doi.org/10.1016/0921-5107(94)01176-1.

Lin, D.-Z., Chang, H.-I., Tsia, K.-C., Chung, Y.-Y., 2024. Low power density, high-efficiency reflective Raman system for polymer SERS substrates. RSC Adv. 14, 20879. https://doi.org/10.1039/d4ra03874f.

Lin, D.-Y., Tsai, C.-H., Huang, Y., Ye, S.-B., Lin, C.-H., Lee, K.-Y., Wu, M.-H., 2020. Novel strategy for food safety risk management and communication: Risk identification for benzoic acid residues in pickled vegetables. Food Sci. Nutr. 8 (10), 5419–5425. https://doi.org/10.1002/fsn3.1839.

Liu, Y.-J., Chu, H.Y., Zhao, Y.-P., 2010. Silver nanorod array substrates fabricated by oblique angle deposition: morphological, optical, and SERS characterizations. J. Phys. Chem. C. 114, 8176–8183. https://doi.org/10.1021/jp1001644.

Lone, A.B., Bhat, H.F., Kumar, S., Manzoor, M., Hassoun, A., Aït-Kaddour, A., Mungure, T.E., Aadil, R.M., Bhat, Z.F., 2023. Improving microbial and lipid oxidative stability of cheddar cheese using cricket protein hydrolysates pre-treated with microwave and ultrasonication. Food Chem. 423, 136350 https://doi.org/10.1016/j.foodchem.2023.136350.

Long, G.L., Winefordner, J.D., 1983. Limit of detection. A closer look at the IUPAC definition. Anal. Chem. 55, 712A–724A. https://doi.org/10.1021/ac00258a724.

Luo, Y., Jing, Q., Li, C., Liang, A., Wen, G., He, X., Jiang, Z., 2018. Simple and sensitive SERS quantitative analysis of sorbic acid in highly active gold nanosol substrate. Sens. Actuators B: Chem. 255, 3187–3193. https://doi.org/10.1016/j.snb.2017.09.144.

Ma, X., Xu, S., Pan, Y., Jiang, C., Wang, Z., 2024. Construction of SERS output-signal aptasensor using MOF/noble metal nanoparticles based nanozyme for sensitive histamine detection. Food Chem. 440, 138227 https://doi.org/10.1016/j.foodchem.2023.138227.

Mejlholm, O., Dalgaard, P., 2013. Development and validation of an extensive growth and growth boundary model for psychrotolerant Lactobacillus spp. in seafood and meat products. Int. J. Food Microbiol. 167, 244–260. https://doi.org/10.1016/j.ijfoodmicro.2013.09.013.

Mejlholm, O., Kjeldgaard, J., Modberg, A., Vest, M.B., Bøknæs, Koort, N.J., Björkroth, J., Dalgaard, P., 2008. Microbial changes and growth of Listeria monocytogenes during chilled storage of brined shrimp (Pandalus borealis). Int. J. Food Microbiol. 124, 250–259. https://doi.org/10.1016/j.ijfoodmicro.2008.03.022.

Mologoni, L., Valese, A.C., Lorenzetti, A., Daguer, Heitor, Lindner, J.D.D., 2016. Development of a LC–MS/MS method for the simultaneous determination of sorbic acid, natamycin and tylosin in Dulce de leche. Food Chem. 211, 748–756. https://doi.org/10.1016/j.foodchem.2016.05.105.

Moskovits, M., 1985. Surface-enhanced spectroscopy. Rev. Mod. Phys. 57 (3), 783–826. https://doi.org/10.1103/RevModPhys.57.783.

Neng, J., Wang, J., Wang, Y., Zhang, Y., Chen, P., 2023. Trace analysis of food by surface-enhanced Raman spectroscopy combined with molecular imprinting technology: principle, application, challenges, and prospects. Food Chem. 429, 136883 https://doi.org/10.1016/j.foodchem.2023.136883.

Ohtsuki, T., Sato, K., Furusho, N., Kubota, H., Sugimoto, N., Akiyama, H., 2013. Absolute quantification of dehydroacetic acid in processed foods using quantitative ^{1}H NMR. Food Chem. 141 (2), 1322–1327. https://doi.org/10.1016/j.foodchem.2013.04.005.

Ohtsuki, T., Sato, K., Sugimoto, N., Akiyama, H., Kawamura, Y., 2012a. Absolute quantification for benzoic acid in processed foods using quantitative proton nuclear magnetic resonance spectroscopy. Talanta 99, 342–348. https://doi.org/10.1016/j.talanta.2012.05.062.

Ohtsuki, T., Sato, K., Sugimoto, N., Akiyama, H., Kawamura, Y., 2012b. Absolute quantitative analysis for sorbic acid in processed foods using proton nuclear magnetic resonance spectroscopy. Anal. Chim. Acta 734, 54–61. https://doi.org/10.1016/j.aca.2012.04.033.

Olson, L.G., Harris, J.M., 2008. Surface-enhanced Raman spectroscopy studies of surfactant adsorption to a hydrophobic interface. Appl. Spectrosc. 62 (2), 149–156. https://doi.org/10.1366/000370208783575492.

Pagannone, M., Fornari, B., Mattei, G., Lupton, R.A., 1987. Molecular structure and orientation of chemisorbed aromatic carboxylic acids: Surface enhanced Raman spectrum of benzoic acid adsorbed on silver sol. Spectrochim. Acta Part A: Mol. Biomol. Spectrosc. 43, 621–625. https://doi.org/10.1016/0584-8539(87)80143-5.

Pelle, F.D., Scroccarello, A., Sergi, M., Mascini, M., Carlo, M.D., Compagnone, D., 2018. Simple and rapid silver nanoparticles based antioxidant capacity assays: reactivity study for phenolic compounds. Food Chem. 256, 342–349. https://doi.org/10.1016/j.foodchem.2018.02.141.

Qi, M., Wang, B., Jiang, H., Li, Y., Li, P., Zhang, X., H, L., 2024. Smartphone readable colorimetry and surface-enhanced raman scattering (SERS) dual-mode sensing platform for ascorbic acid detection based on GeO2 composite nanozymes. J. Food Compos. Anal. 125, 105740 https://doi.org/10.1016/j.jfca.2023.105740.

Robbie, K., Beydaghyan, G., Brown, T., Dean, C., Adams, J., Buzea, C., 2004. Ultrahigh vacuum glancing angle deposition system for thin films with controlled three-dimensional nanoscale structure, 1089–1097-1089 Rev. Sci. Instrum. 75. https://doi.org/10.1063/1.1667254.

Saad, B., Bari, Md.F., Saleh, Ahmad, M.I.K., Talib, M.K.M., 2005. Simultaneous determination of preservatives (benzoic acid, sorbic acid, methylparaben and

propylparaben) in foodstuffs using high-performance liquid chromatography. J. Chromatogr. A 1073 (1–2). https://doi.org/10.1016/j.chroma.2004.10.105.
Saraiva, G.D., Nogueira, C.E.S., Freire, P.T.C., de Sousa, F.F., da Silva, J.H., Teixeira, A. M.R., 2015. Temperature-dependent vibrational spectroscopic study and DFT calculations of the sorbic acid. Spectrochim. Acta Part A: Mol. Biomol. Spectrosc. 137, 1409–1416. https://doi.org/10.1016/j.saa.2014.08.142.
Shrivas, K., Nirmalkar, N., Thakur, S.S., Deb, M.K., Shinde, S.S., Shankar, R., 2018. Sucrose capped gold nanoparticles as a plasmonic chemical sensor based on non-covalent interactions: Application for selective detection of vitamins B1 and B6 in brown and white rice food samples. Food Chem. 250, 14–21. https://doi.org/10.1016/j.foodchem.2018.01.002.
Sirhan, A.Y., 2018. Optimization and validation of an HPLC-UV method for determination of benzoic acid and sorbic acid in yogurt and dried-yogurt products using a design of experiment. Indones. J. Chem. 18 (3), 522–530. https://doi.org/10.22146/ijc.27675.
Stiles, P.L., Dieringer, J.A., Shah, N.C., Duyne, R.P.V., 2008. Surface-enhanced Raman spectroscopy. Annu. Rev. Anal. Chem. 1, 601–626. https://doi.org/10.1146/annurev.anchem.1.031207.112814.
Tsen, C.-M., Yu, C.-W., Chen, S.-Y., Lin, C.-L., Chuang, C.-Y., 2021. Application of surface-enhanced Raman scattering in rapid detection of dithiocarbamate pesticide residues in foods. Appl. Surf. Sci. 558, 149740 https://doi.org/10.1016/j.apsusc.2021.149740.
Tsen, C.-M., Yu, C.-W., Chuang, W.-C., Chen, M.-J., Lin, S.-K., Shyu, T.-H., Wang, Y.-H., Li, C.-C., Chao, W.-C., Chuang, C.-Y., 2018. A simple approach for the ultrasensitive detection of paraquat residue in adzuki beans by surface-enhanced Raman scattering. Analyst 144, 426–438. https://doi.org/10.1039/C8AN01845F.
Vosgröne, T., Meixner, A.J., 2005. Surface and resonance enhanced micro-Raman spectroscopy of Xanthene Dyes: from the ensemble to single molecules. Chempyhschem 6, 154–163. https://doi.org/10.1002/cphc.200400395.
Waiwijit, U., Chananonnawathorn, C., Eimchai, P., Bora, T., Hornyak, G.L., Nuntawong, N., 2020. Fabrication of Au-Ag nanorod SERS substrates by co-sputtering technique and dealloying with selective chemical etching. Appl. Surf. Sci. 530, 147171 https://doi.org/10.1016/j.apsusc.2020.147171.
Wei, R., Li, W., Yang, L., Jiang, Y., Xie, T., 2011. Online preconcentration in capillary electrophoresis with contactless conductivity detection for sensitive determination of sorbic and benzoic acids in soy sauce. Talanta 83 (5), 1487–1490. https://doi.org/10.1016/j.talanta.2010.11.036.
Wu, Y.-T., Yang, C.-E., Ko, C.-H., Wang, Y.-N., Liu, C.-C., Fu, L.-M., 2020. Microfluidic detection platform with integrated micro-spectrometer system. Chem. Eng. J. 393, 124700 https://doi.org/10.1016/j.cej.2020.124700.
Yang, Z., Ma, C., Gu, J., Wu, Y., Zhu, C., Li, L., Gao, H., Yin, W., Wang, Z., Zhang, Y., Shang, Y., Wang, C., Chen, G., 2022. SERS detection of benzoic acid in milk by using Ag-COF SERS substrate. Spectrochim. Acta, Part A: Mol. Biomol. Spectrosc. 267, 120534 https://doi.org/10.1016/j.saa.2021.120534.
Zhang, Z.-M., Chen, S., Liang, Y.-Z., 2010. Baseline correction using adaptive iteratively reweighted penalized least squares. Analyst 135, 1138–1146. https://doi.org/10.1039/B922045C.
Zhang, Y., Yang, Z., Zou, Y., Farooq, S., Li, Y., Zhang, H., 2023. Novel Ag-coated nanofibers prepared by electrospraying as a SERS platform for ultrasensitive and selective detection of nitrite in food. Food Chem. 412, 135563 https://doi.org/10.1016/j.foodchem.2023.135563.
Zhao, X., Fang, Y., 2006. Raman experimental and DFT theoretical studies on the adsorption behavior of benzoic acid on silver nanoparticles. J. Mol. Struct. 789, 157–161. https://doi.org/10.1016/j.molstruc.2005.12.049.